

COVER SHEET

Title: *Sensing Resolution and Measurement Range of a Passive Wireless Strain Sensor*

Authors: Xiaohua Yi
Terence Wu
Gabriel Lantz
James Cooper
Chunhee Cho
Yang Wang
Manos M. Tentzeris
Roberto T. Leon

ABSTRACT

In this research, folded patch antennas are explored for the development of low-cost and wireless smart-skin sensors that monitor the strain in metallic structures. When the patch antenna is under strain/deformation, its resonance frequency varies accordingly. The variation can be easily interrogated and recorded by a wireless reader that also wirelessly delivers power for the antenna operation. The patch antenna adopts a specially selected substrate material with low dielectric constant, as well as an inexpensive off-the-shelf radiofrequency identification (RFID) chip for signal modulation. This paper reports latest tensile test results on the strain sensing limit of the prototype folded patch antenna. In particular, it is shown that the passive wireless sensor can detect small strain changes lower than $20 \mu\epsilon$, and can perform well at a strain range higher than $10,000 \mu\epsilon$.

INTRODUCTION

Nearly one third of the 604,426 bridges in the U.S. are made of steel and aluminum iron, among which almost 20% are rated as structurally deficient and 17.7% functionally obsolete [1]. For all deficient bridges, fatigue-induced fracture/crack is among the most common concerns for inspectors and owners [2]. Current biennial bridge deck evaluation and assessment methods are mainly based on visual inspection [3], which cannot detect small-size cracks hidden under paint. The cracks may grow to critical and dangerous sizes before the next inspection cycle. Early detection of cracks for fracture-critical-members of steel bridges has long been a challenging issue in bridge health monitoring. Some existing technologies, including metal foil strain gages, fiber optic sensors, or ultrasonic testing, may assist in crack monitoring. However, most sensing systems either require running lengthy cables in the structure

Xiaohua Yi, Gabriel Lantz, Chunhee Cho, Yang Wang and Roberto T. Leon, School of Civil and Environmental Engineering, Georgia Institute of Technology, Atlanta, GA 30332, USA
Terence Wu, James Cooper and Manos M. Tentzeris, School of Electrical and Computer Engineering, Georgia Institute of Technology, Atlanta, GA 30332, USA

[4], or cover only very limited areas of the structure, or involve human-operated equipment that is not convenient for in-situ continuous application. As a result, these technologies suffer from their high instrumentation and monitoring cost and are not practical for large-scale/large-area deployment and continuous monitoring in the field.

This research investigates a different approach of exploiting wireless electromagnetic (EM) waves for strain sensing through the development of “smart skins” made of radiofrequency identification (RFID)-enabled patch antennas. The dimension-dependent behavior of EM waves with the antenna is exploited as the sensing mechanism. The basic concept is that when a small piece of antenna (usually with 2D shape) is under strain/deformation, its EM resonance frequency can change accordingly. Such change can be interrogated by a wireless reader and used as a strain indicator. Loh *et al.* [5] developed inductively coupled wireless strain sensors to measure the shift of resonance frequency under tensile strain, which shows an approximately relationship. Chen *et al.* [6] successfully developed corrosion sensors using the same inductive coupling concept. One drawback of inductively coupling, however, is that the interrogation distance is usually limited.

To overcome the limitations in interrogation distance, EM backscattering systems can provide an alternative [7]. For example, Deshmukh and Huang [8] developed a microstrip patch antenna for measuring strain and detecting cracks in metallic structures. In addition, Thomson *et al.* [9] developed a wireless strain sensor based on RF cavity. The RF cavity sensor achieved an interrogation distance of 8m, but the system requires an external regular antenna being connected outside the cavity at the sensor side. More recently, Yi *et al.* [10] developed an RFID-based folded patch antenna as a passive wireless strain sensor for metallic structures. The system utilizes the principle of EM backscattering and adopts a low-cost off-the-shelf RFID chip to reduce the design and manufacturing cost. The RFID-based technology allows the sensor to be passive, i.e. to operate without other power source such as batteries [11]. Instead, the sensor receives operation energy entirely from the wireless transmission by the reader. Through experiments, the strain sensing resolution is previously demonstrated to be under 50 $\mu\epsilon$, and the wireless interrogation distance is shown to be over a few feet for this preliminary prototype.

In this research, the strain sensing resolution and measurement range of the prototype sensor are further investigated. Both parameters are important metrics for practical deployment of the sensor. An extensive suite of tensile tests are devised and conducted to characterize the strain sensing performance. The rest of the paper is organized as follows. First, the design and manufacturing of the prototype wireless strain sensor are summarized. The operation principle of the system is then described. Experimental results are presented illustrating excellent sensing performance in terms of strain resolution and measurement range. Finally, a summary and discussion of this work are provided.

STRAIN SENSING PRINCIPLE

As shown in Fig.1, the passive wireless strain sensing system consists of an RFID reader and an RFID tag (i.e. wireless strain sensor), where the tag includes an antenna and an integrated circuit (IC) chip. The operation of the system is based on EM backscattering. The reader emits interrogation EM wave to the tag at power level P_1 . If the power received by the tag is larger than the activation power threshold of the

IC chip, the tag is activated and reflects EM wave back to the reader at power level P_2 . The first subsection introduces the RFID tag design and the basic formulation for its resonance frequency. The procedure for extracting the resonance frequency from the reader measurement is described afterward.

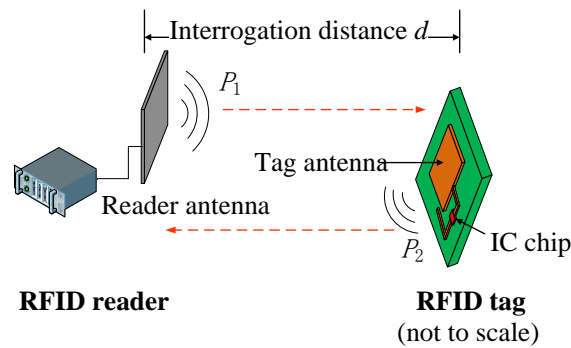


Fig.1. Power transmission and backscattering in a passive RFID tag-reader system

RFID Tag Design

The RFID tag developed in this research utilizes RFID IC chips that usually have very small feature sizes and are inexpensive to produce. The RFID IC chip for this application is chosen as the SL3ICS1002 model from NXP Semiconductors. The dimension of the chip, excluding the size of the pads for soldering, is $1 \text{ mm} \times 1 \text{ mm}$. The impedance of the chip is $13.3-j122 \Omega$ (“ j ” is the imaginary unit), which is low and relatively easy to match during the tag antenna design. The broad operating frequency range of the chip (from 840 MHz to 960 MHz) allows international usage.

The design drawing and picture of this prototype are shown in Fig. 2. Both the design drawing and the picture illustrate the front/top side of the RFID tag, where the IC chip is soldered on patterned copper cladding (as the conducting component of the tag antenna). The dimension for each part is shown in this figure too. The adopted substrate material is Rogers RT/duroid[®]5880, a glass microfiber reinforced poly-tetrafluoro-ethylene (PTFE) composite with a dielectric constant ϵ_r of 2.20 and a thickness of 31 mils (0.79 mm). The RT/duroid[®]5880 material is used due to its low dielectric attenuation, which improves the interrogation range and the quality factor of the RFID tag. Furthermore, glass microfiber reinforced composites have more reliable mechanical behavior under strain compared with ceramic-filled composites that can be used for other antenna applications. Vias through the substrate are used for connecting the top copper cladding with the ground plane on the back of the substrate, forming a folded patch antenna. One pin of the IC chip is also connected with the ground plane through a via.

The RFID tag design is based on a quarter-wave rectangular patch antenna (folded-patch) topology [7]. The topology is chosen for its good radiation performance on top of metallic objects, and because it enables 50% reduction to the footprint as compared with a regular patch antenna. The antenna resonance frequency at zero strain level, f_{R0} , can be estimated as:

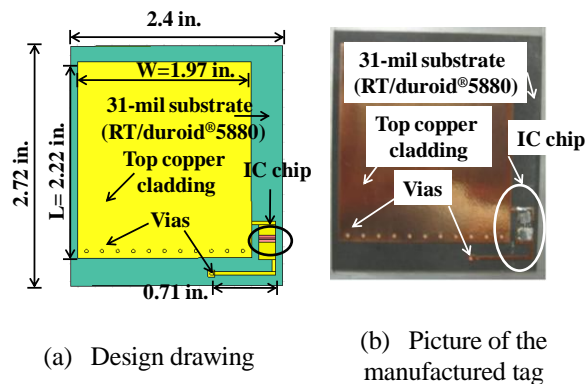


Fig. 2. RFID tag as wireless strain sensor

$$f_{R0} = \frac{c}{4(L+L')\sqrt{\epsilon_r}} \quad (1)$$

where c is the speed of light; L is the physical length of the top copper cladding (2.22 in. for this design); L' is the additional electrical length compensating the fringing effect. When the antenna experiences strain deformation of ϵ in the longitudinal direction, the resonance frequency shifts to:

$$f_R = \frac{c}{4(1+\epsilon)(L+L')\sqrt{\epsilon_r}} = \frac{f_{R0}}{1+\epsilon} \quad (2)$$

When strain ϵ is small, the resonance frequency changes approximately linearly with respect to strain:

$$f_R = f_{R0}(1 - \epsilon + \epsilon^2 - \epsilon^3 + \dots) \approx f_{R0}(1 - \epsilon) \quad (3)$$

This approximately linear relationship indicates that by measuring the antenna resonance frequency, the applied strain can be derived.

Measurement of Resonance Frequency

The RFID reader (Fig.1) adopted in this application is the Tagformance unit from Voyantic. The reader can sweep through an interrogation frequency range from 800 MHz to 1000 MHz at a frequency resolution of 0.1 MHz. At each interrogation frequency, the reader emits different levels of power in order to identify the transmitted power threshold (least transmitted power required to activate the IC chip). The power measurement resolution is 0.1 dBm. Through a USB 2.0 port, a computer interface is used to operate and retrieve measurement data from the reader.

The RFID tag antenna has been designed with one specific resonance frequency, which provides best impedance matching between the tag antenna and the IC chip. When the interrogation frequency f of reader is equal to the resonance frequency of the RFID tag, the least amount of power needs to be transmitted by the reader for activating the RFID tag. This means the transmitted power threshold plot $P_1(f)$ (measured by the reader) reaches minimum value at the resonance frequency, which is shown in Fig. 3. When there is no strain/deformation, the minimum occurs at resonance frequency f_{R0} (Eq. (1)). When the antenna length changes due to strain ϵ in the longitudinal direction, the resonance frequency changes accordingly to f_R (Eq. (2)), and the $P_1(f)$ plot for the antenna under strain reaches minimum at f_R .

INVESTIGATION ON WIRELESS STRAIN SENSING RESOLUTION

Preliminary study on the strain sensing performance of the prototype sensor has been presented in [10]. The strain sensing results demonstrate good linearity at 50 $\mu\epsilon$ resolution. To explore the performance limit in strain resolution, similar test is conducted with reduced strain increment per loading step. Fig. 4(a) shows the center area of the tensile testing specimen, with the wireless strain sensor and seven conventional strain gages measuring the axial strain on the aluminum

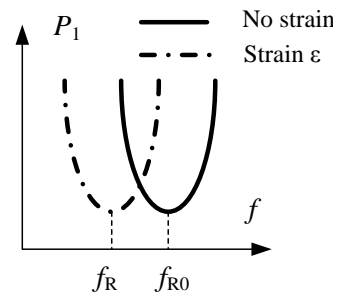


Fig. 3. Conceptual illustration of resonance frequency shift due to strain

specimen. Fig. 4 (b) shows the experimental setup for the tensile testing with a 22-kip SATEC machine. The reader antenna is mounted on a tripod facing the wireless strain sensor. The distance between the reader antenna and the wireless sensor is set as 12 in. Through a coaxial cable, the reader antenna is connected with the Tagformance reader. A National Instruments strain gage module (NI 9235), in combination with a CompactDAQ Chassis (NI cDAQ-9172), is used for collecting data from conventional metal foil strain gages.

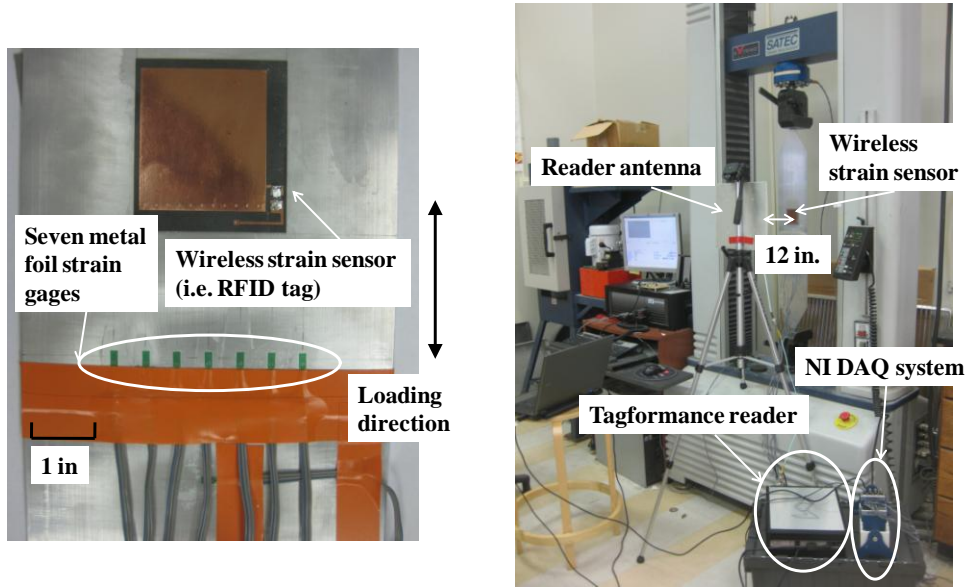
The force applied by the testing machine is configured so that approximately a $20 \mu\epsilon$ increment is achieved at each loading step. The average interrogation power threshold in dBm scale, $\underline{P}_1(f)$, is measured by the Tagformance reader at each loading step. Assuming P_1 is the power threshold in milliwatt, the conversion to dBm scale is defined as:

$$\underline{P}_1 = 10 \log_{10} P_1 \quad (4)$$

To reduce the effect of measurement noise, five measurements are taken for each strain level and the average is calculated at every interrogation frequency f :

$$\overline{P}_1(f) = \frac{1}{5} \sum_{i=1}^5 [\underline{P}_1^i(f)] \quad (5)$$

where \overline{P}_1 is the average transmitted power threshold in dBm, $\underline{P}_1^i(f)$ is the transmitted power threshold in dBm from the i^{th} measurement. For clarity, the average transmitted power threshold at $11 \mu\epsilon$, $101 \mu\epsilon$, and $193 \mu\epsilon$ are plotted in Fig. 5(a). The strain levels are calculated as the average among the seven axial strain gages. A clear resonance frequency shift is observed as strain increases. As described in the last section, the transmitted power threshold reaches its minimum value at the resonance frequency. A 4th order polynomial curve fitting is performed to the valley area of the $\overline{P}_1(f)$ plot at each strain level [10]. The value of the fitted 4th order polynomial is re-calculated at a frequency step of 0.001 MHz for identifying the resonance frequency.



(a) Picture of the sensor instrumentation for wireless sensing experiments

(b) Picture of the experimental setup

Fig. 4. Experimental setup for the tensile tests

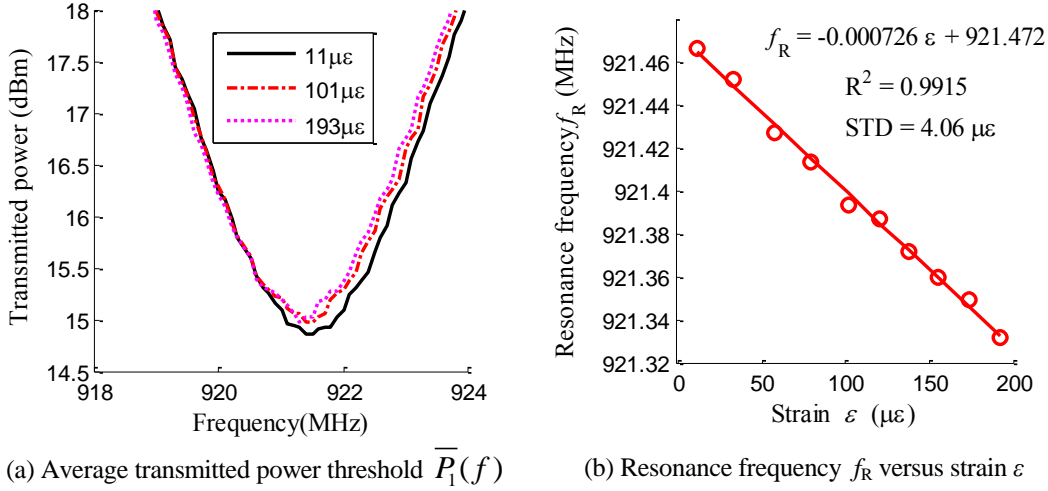


Fig. 5. Tensile testing results for the $\sim 20 \mu\epsilon/\text{step}$ loading case at 12 in. interrogation distance

The resonance frequency f_R , as determined through the 4th order curve fitting, is plotted in Fig. 5(b) against the strain level. The ten data points correspond to ten strain levels. As a result of linear regression, the slope parameter is identified as $-726 \text{ Hz}/\mu\epsilon$ (i.e. $-0.000726 \text{ MHz}/\mu\epsilon$). This parameter corresponds to the strain sensitivity of the wireless sensor, which means that $1 \mu\epsilon$ increment in the aluminum specimen causes 726 Hz decrease in the resonance frequency of the wireless strain sensor. According to Eq. (1) and the tag antenna dimensions provided in Fig. 2, the theoretical resonance frequency of the sensor at zero strain level can be estimated in SI units as:

$$f_{R0} = \frac{3 \times 10^8}{4 \times (54.5 + 0.414) \times 10^3 \times \sqrt{2.2}} = 920.8 \text{ MHz} \quad (6)$$

The relative difference between the theoretical and the experimental resonance frequency f_{R0} is within 0.1%, which shows a very close match. According to Eq. (3), theoretically, the approximate strain sensitivity should equal to f_{R0} , i.e., $-920.8 \text{ Hz}/\mu\epsilon$. The difference between the analytical and experimental strain sensitivities is partly due to the strain transfer from the aluminum specimen to the top copper cladding. Since the thickness of the RFID tag is over 30 mils, the strain experienced by the top copper cladding is smaller than the strain occurring in the aluminum specimen (as measured by the strain gages). This strain transfer process reduces the strain sensitivity of the prototype sensor. In addition, the dielectric constant ϵ_r (which is assumed constant in the analytical study) also changes with respect to strain. Different from an ideal material, small voids always exist in the substrate. Distortion of the voids under strain can affect ϵ_r . The dielectric constant change due to strain requires in-depth studies in the future.

Fig. 5(b) also shows the coefficient of determination, R^2 , from the linear regression [12]. A value of $R^2 = 0.9915$ indicates a good level of linearity. In order to further check the accuracy of the measurements, the standard deviation of the measurement error is calculated as:

$$STD = \sqrt{\frac{1}{N-1} \sum_{i=1}^N (\Delta \varepsilon_i)^2} \quad (7)$$

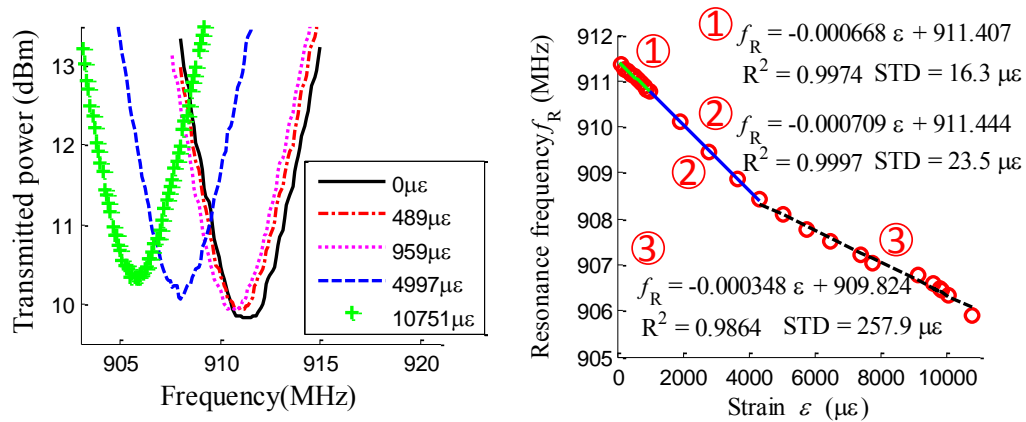
where $\Delta \varepsilon_i$ is the difference between the measured strain and the strain estimated using the linear relationship at the i^{th} strain level, N is the total number of strain levels. As

shown in Fig. 5(b), the standard deviation is $4.06 \mu\epsilon$, which shows an acceptable accuracy for such a passive wireless strain sensor.

INVESTIGATION ON THE MEASUREMENT RANGE OF THE WIRELESS STRAIN SENSOR

Similar experiment is performed to explore the range of the proposed prototype sensor. The measurement range experiment is conducted on a MTS-810 tensile testing machine, which has a capacity of 55 kips. Most of the experimental setup is similar to the previous experiments for strain sensing resolution, except for the loading control and steps. During this experiment, the displacement control mode is adopted for the testing machine, because the aluminum specimen is expected to yield during the experiment. From 0 to $1,000 \mu\epsilon$, each loading step is configured to increase the strain level by about $100 \mu\epsilon$; from $1,000 \mu\epsilon$ to $10,000 \mu\epsilon$, each loading step generates a strain increment of about $1,000 \mu\epsilon$.

The average transmitted power threshold at different strain levels are shown in Fig. 6(a). For clarity, only five example strain levels are shown in the figure. The resonance frequency f_R is plotted in Fig. 6(b) against the strain level. Separate linear regression is conducted to three segments of the plot. For segment ① with data points from 0 to $1,000 \mu\epsilon$, the sensitivity slope is $-668 \text{ Hz}/\mu\epsilon$. For segment ② with data points from $1,000$ to $4,500 \mu\epsilon$, the sensitivity slope is $-709 \text{ Hz}/\mu\epsilon$, which is slightly higher. The slightly different slope can be explained by Eq. (3), which shows that the approximate linearity becomes weaker as strain increases. For segment ③, the relatively low sensitivity is due to the yielding of both the aluminum specimen and the copper antenna, as well as the dielectric property change of the Rogers 5880 substrate. The coefficients of determination at these three segments are 0.9974, 0.9997, and 0.9864, respectively. The standard deviations for the first two segments are much smaller than the third segment, due to more linear material property at lower strain level.



(a) Average transmitted power threshold $\overline{P}_1(f)$ (b) Resonance frequency f_R versus strain ϵ

Fig. 6. Tensile testing results for the strain sensing range case at 12 in. interrogation distance

SUMMARY AND DISCUSSION

This paper presents the strain sensing resolution and measurement range of a prototype wireless strain sensor, whose design is based on a folded patch antenna. Both analytical studies and tensile testing experiments demonstrate an approximately linear relationship between the resonance frequency of the antenna and the strain experienced by the sensor, particularly at small strain levels. It is shown that the passive wireless sensor can detect small strain changes lower than 20 $\mu\epsilon$, and can perform well at a strain range higher than 10,000 $\mu\epsilon$.

Since the resonance frequency of the wireless strain sensor is correlated with the size of the patch antenna, the footprint of the sensor can be significantly reduced in future studies by increasing the operating frequency. In addition, longer interrogation distance can be achieved by adopting a high gain antenna or increasing the transmitted power at the reader side.

ACKNOWLEDGEMENT

This material is based upon work supported by the Federal Highway Administration under agreement No. DTFH61-10-H-00004. Any opinions, findings, and conclusions or recommendations expressed in this publication are those of the authors and do not necessarily reflect the view of the Federal Highway Administration.

REFERENCES

1. FHWA. 2011. *National Bridge Inventory*. U.S. Department of Transportation, Federal Highway Administration, Washington D.C.
2. ASCE. 2009. *Report Card for America's Infrastructure*. American Society of Civil Engineers, Reston, VA.
3. AASHTO. 2009. *Manual of Bridge Evaluation*. American Association of State Highway & Transportation Officials, Washington D.C.
4. Çelebi, M. 2002. *Seismic Instrumentation of Buildings (with Emphasis on Federal Buildings)*. Report No. 0-7460-68170, United States Geological Survey, Menlo Park, CA.
5. Loh, K.J., J.P. Lynch, and N.A. Kotov. 2008. "Inductively coupled nanocomposite wireless strain and pH sensors," *Smart Struct. Syst.*, **4**(5):531-548.
6. Chen, Y., S. Munukutla, P. Pasupathy, D.P. Neikirk, and S.L. Wood. 2010. "Magneto-inductive waveguide as a passive wireless sensor net for structural health monitoring," *Proc. SPIE, Sensor and Smart Structures Technologies for Civil, Mechanical, and Aerospace Systems 2010*, March 8, 2010.
7. Finkenzeller, K. 2003. *RFID Handbook*. Wiley, New York.
8. Deshmukh, S. and H. Huang. 2010. "Wireless interrogation of passive antenna sensors," *Meas. Sci. Technol.*, **21**(3):035201.
9. Thomson, D.J., D. Card, and G.E. Bridges. 2009. "RF cavity passive wireless sensors with time-domain gating-based interrogation for SHM of civil structures," *IEEE Sensors J.*, **9**(11):1430-1438.
10. Yi, X., T. Wu, Y. Wang, R.T. Leon, M.M. Tentzeris, and G. Lantz. 2011. "Passive wireless smart-skin sensor using RFID-based folded patch antennas," *Int. J. Smart Nano Mater.*, **2**(1):22-38.
11. Balanis, C.A. 1997. *Antenna Theory: Analysis and Design*. John Wiley and Sons Inc., New York.
12. Chatterjee, S. and A.S. Hadi. 1986. "Influential observations, high leverage points, and outliers in linear regression," *Stat. Sci.*, **1**(3):379-416.